Received: 6 March 2023 | Accepted: 25 June 2023

DOI: 10.1002/jpln.202300071

RESEARCH ARTICLE

Silencing of *FRO1* gene affects iron homeostasis and nutrient balance in tomato plants

Florinda Gama[1,2] | **Teresa Saavedra**[1] | **Susana Dandlen**[1] | **Pedro García-Caparrós**[3] | **Amarilis de Varennes**[4] | **Gustavo Nolasco**[5] | **Pedro José Correia**[1] | **Maribela Pestana**[1]

[1]MED, —Mediterranean Institute for Agriculture, Environment and Development and CHANGE—Global Change and Sustainability Institute, Faculty of Science and Technology, University of Algarve, Faro, Portugal

[2]GreenCoLab—Associação Oceano Verde, University of Algarve, Faro, Portugal

[3]Agronomy Department of Superior School Engineering, University of Almeria, Almeria, Spain

[4]Instituto Superior de Agronomia, University of Lisbon, Lisbon, Portugal

[5]Faculty of Science and Technology, University of Algarve, Faro, Portugal

Correspondence
Maribela Pestana, MED—Mediterranean Institute for Agriculture, Environment and Development and CHANGE—Global Change and Sustainability Institute, Faculty of Science and Technology, University of Algarve, Building 8, Campus of Gambelas, 8005-139 Faro, Portugal.
Email: fpestana@ualg.pt

This article has been edited by Michael Frei.

Funding information
National Project, Grant/Award Number: PTDC/AGR-PRO/3861/2012

Abstract

Background: Iron chlorosis is an abiotic stress of worldwide importance affecting several agronomic crops. It is important to understand how plants maintain nutrient homeostasis under Fe deficiency and recovery.

Aims: We used the virus-induced gene silencing (VIGS) method to elucidate the role of the *FRO1* gene in tomato plants and identify the impact on regulation of the root ferric-chelate reductase (FCR) activity and nutritional homeostasis.

Methods: Tomato plantlets cv. "Cherry" were transferred into half-strength Hoagland's nutrient solution containing 0.5 μM of Fe (Fe0.5). In phase I, two treatments were established: control (Fe0.5) plants and VIGS-0.5 plants corresponding to plants with the *FRO1* gene silenced. In phase II, plants from Fe0.5 and VIGS-0.5 were transferred to new nutrient solution and then grown for a further 14 days under 0 and 10 μM of Fe (as 0.5 μM would not be enough for the larger plants during phase II). Therefore, four treatments were imposed: Fe0, Fe10, VIGS-0, and VIGS-10.

Results: VIGS-0.5 plants had significantly lower chlorophyll (Chl) and root FCR activity compared to the respective non-silenced plants and retained more Cu and Zn in the roots at the expense of stems (Cu) or young leaves (Zn). Iron concentration in roots and stems decreased in *FRO1* gene-silenced plants, compared to control plants, but the allocation to different organs was similar in both treatments.

Conclusions: There was a partial recovery of leaf Chl in the VIGS-10 plants and a higher concentration of Fe in all organs. In contrast, the allocation of Cu to roots decreased in the VIGS-10 plants.

KEYWORDS
ferric-chelate reductase, iron deficiency, iron homeostasis, nutrients, virus-induced gene silencing

1 | INTRODUCTION

One of the most frequent abiotic stresses affecting crops grown in calcareous soils is restricted iron (Fe) uptake, and the consequent leaf chlorosis. Iron is an essential plant micronutrient and plays a crucial role in several metabolic processes that depend on adequate Fe levels in plant tissues, such as chlorophyll biosynthesis, respiration, and photosynthesis (Abadía et al., 2011).

Given the narrow range of Fe concentrations required, plants must have well-tuned systems to ensure adequate internal Fe concentrations (Murgia et al., 2022). Excess of Fe can be harmful due to the overproduction of reactive oxygen species, which causes cellular damage resulting in browning spots in leaves (Zahra et al., 2021). Conversely, under Fe deficiency, plants have different strategies to ensure Fe uptake: a reduction strategy (Strategy I) for all species except grasses, a complexing strategy (Strategy II) defined by the ability

of grasses to exudate Fe chelators and take up intact Fe(III) phytosiderophores complexes into root cells, and a combined strategy exhibited in rice plants (Marschner et al., 1986; Ricachenevsky & Sperotto, 2014; Schmid et al., 2014). However, recently the boundaries between these strategies have been questioned. Under Fe deficiency, dicots may also exudate potent Fe-complexing compounds (Rajniak et al., 2018), and grasses may have a reducing Fe capacity (Nozoye et al., 2017). This new approach has a relevant impact on Fe nutrition, especially on Fe uptake strategies.

Tomato plants have been used as model crop to study the molecular mechanisms of Fe uptake in Strategy I plants (Du et al., 2015; Graziano & Lamattina, 2007; Sahu et al., 2012), which comprise the acidification of the rhizosphere by extrusion of H^+, the reduction of Fe(III) to Fe(II) by the enzyme ferric-chelate reductase (FCR) located in the plasma membrane of the root epidermal cells and the uptake of Fe(II) in epidermal cells by the iron-regulated transporter (Walker & Connolly, 2008).

Once inside the plant, there is a long journey for Fe, from root to seed, which was described in detail by Murgia et al. (2022). During this pathway, the (FCR) is responsible for Fe reduction (Barberon et al., 2014; Connolly et al., 2003; Kobayashi & Nishizawa, 2012; Robinson et al., 1999; Walker & Connolly, 2008), especially in dicots. Its expression levels are determined by the ferric reductase oxidase gene (*FRO1*) (Ivanov et al., 2012; Jain et al., 2014; Jeong & Connolly, 2009; Mukherjee et al., 2006). The role of the *FRO* family of metal reductases in Fe homeostasis is essential in the process of reduction and uptake of Fe (Bernal et al., 2012). Additionally, the members of *FRO* family have functional roles in several subcellular compartments, such as chloroplast and vacuole membranes (Jain et al., 2014; Li et al., 2019). According to Grotz and Guerinot (2006), *LeFRO1* mRNA is also detected in shoots regardless of Fe status, suggesting that *LeFRO1* may play a role in Fe mobilization in the shoots as well.

To understand the molecular regulation of nutritional balances in chlorotic Fe plants, traditional approaches, such as mutant screening and plant transformation, were normally used, but they are often time-consuming and labor-intensive (Fu et al., 2016). On the other hand, obtaining a transgenic plant is complex and not suitable for the functional characterization of many genes. Virus-induced gene silencing (VIGS) is an effective method to study many genes in plants because it is simple, fast, and efficient, and it does not rely on genetic transformation, among other advantages. VIGS can be used to knock-down individual plant genes and study the effects of their inactivation on plant phenotypes (Becker & Lange, 2010; Burch-Smith et al., 2004; Gama et al., 2017; He et al., 2008; Lange et al., 2013; Lu et al., 2003; Senthil-Kumar & Myosore, 2011).

One of the most widely used vectors for VIGS is tobacco rattle virus (TRV) because of its ability to infect a wide range of host plants, systemic spread throughout the host plant, including meristematic tissues, and absence of severe symptoms associated with virus disease (Singh et al., 2022). TRV is a positive single-stranded RNA virus with a bipartite genome (RNA1 and RNA2). The pTRV-RNA1 contains the genes required for viral replication and movement, and the pTRV-RNA2 encodes the proteins necessary for virion formation. A partial sequence of the target gene can thus be cloned into a cDNA of pTRV-RNA2 with a multiple cloning site (Sahu et al., 2012; Senthil-Kumar & Mysore, 2011). The expression of the partial sequence will cause the degradation of the mRNA derived from the plant's copy of the gene through the silencing mechanism called posttranscriptional gene silencing, which targets double-stranded RNA often used to suppress viral proliferation and replication.

VIGS has been successfully used in several species for functional analysis of stress-responsive genes involved in abiotic stress of plants like *Nicotiana benthamiana* (Gama et al., 2017; Senthil-Kumar et al., 2008), pepper (Tian et al., 2014), chili pepper (Arce-Rodriguez & Ochoa-Alejo, 2015), potato (Brigneti et al., 2004), citrus (Agüero et al., 2014), and strawberry (Chai et al., 2011) plants. For a recent review see Singh et al. (2019).

The level of tolerance to Fe deficiency is coupled to nutritional balance between different plant organs, not only of Fe, but of other nutrients involved in plant metabolism (Vigani et al., 2017). In addition to all signaling mechanisms for an adequate level of Fe already described in the literature, a question remains: could a change in the Fe reduction process affect the entire nutritional balance of the plant? Our previous work showed that VIGS technique was effective in silencing the *FRO1* gene in *N. benthamiana*; however, the duration of this effect and the possibility of recovery from iron chlorosis by the addition of Fe have not been studied. In the present work, we studied how silencing the *FRO1* gene induces Fe chlorosis, and we assessed the impact of this silencing on the nutrient balance of chlorotic and recovered tomato plants. Understanding the complexities of interaction between Fe and other nutrients would facilitate the implementation of plant growth strategies on soils with low Fe levels with consequences for agricultural production.

2 | MATERIALS AND METHODS

2.1 | Plant material

Tomato (*Solanum lycopersicum* L. cv. "Cherry") seeds were germinated at 25°C in a growth chamber under 16 h/8 h light/dark cycles in a mixture of vermiculite and peat (1:2 v/v). Seedlings with the first two fully expanded leaves were transferred to a glasshouse, under natural photoperiod conditions (October–November) and air temperature ≤25°C. The seedlings were cultivated in 20-L plastic containers (10 plants per container) with aerated half-strength Hoagland's nutrient solution with the following composition: (in mM): $2.5Ca(NO_3)_2{\bullet}4H_2O$, $2.5KNO_3$, $0.5KH_2PO_4$, $1MgSO_4{\bullet}7H_2O$, and (in μM): $23H_3BO_3$, $0.4ZnSO_4{\bullet}7H_2O$, $0.2CuSO_4{\bullet}5H_2O$, $4.5MnCl_2{\bullet}4H_2O$, and 0.01 $(NH_4)_6Mo_7O_{27}{\bullet}H_2O$. At this stage, the adequate concentration of Fe in the nutrient solution, added as Fe-EDDHA, was 0.5 μM of Fe. The pH of the nutrient solution was adjusted to 6.0 ± 0.1 and the electrical conductivity was 1.1 ± 0.1 dS m^{-1}. The plants were left to grow in these conditions for 4 weeks. When the plants had

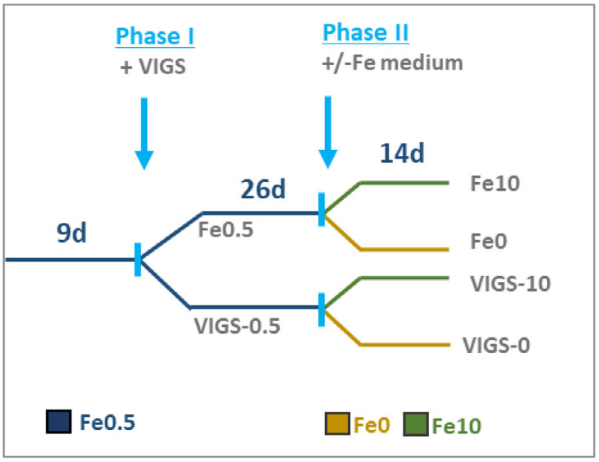

FIGURE 1 Scheme of the experiment indicating the duration of each phase. Phase I—treatments are Fe0.5 (control plants; 0.5 μM of Fe) and virus-induced gene silencing (VIGS)-0.5 (silenced plants; 0.5 μM of Fe). Phase II—treatments are Fe0 (no iron), Fe10 (10 μM of Fe), VIGS-0 (silenced plants; no iron), and VIGS-10 (silenced plants; 10 μM of Fe).

six completely developed leaves, the nutrient solution was changed to full-strength Hoagland nutrient solution (pH = 6.0 ± 0.1 and EC = 2.0 ± 0.2 dS m^{-1}). The nutrient solution was renewed twice over the experimental period.

The experiment had two successive phases (Figure 1), with the following general objectives: (1) phase I, the assessment of the silencing of the *FRO1* gene, and (2) phase II, the impact of previous silencing on the recovery from Fe chlorosis in tomato plants.

In phase I, Fe was added at a concentration of 0.5 μM to all containers and 50 plants were divided into two treatments: (1) Fe0.5: control plants without any vector inoculation, (2) VIGS-0.5: *LeFRO1* silenced plants inoculated with the VIGS vector. The inoculations of the VIGS vector were performed 9 days after the plants were transferred to the full nutrient solution, and in this study, we consider the inoculation date as day 1. After 26 days, five plants from each treatment were harvested for analysis. Phase II started at this date using the remaining silenced and non-silenced plants, which were grown under two levels of Fe (0 and 10 μM of Fe) in renewed full-strength Hoagland's nutrient solutions (pH = 6.0 ± 0.1; EC = 2.0 ± 0.2 dS m^{-1}).

Tomato plants have different nutritional requirements as they grow, and therefore in phase II the concentration of Fe for the sufficiency condition (without chlorosis) had to be adjusted from 0.5 μM (phase I) to 10 μM (phase II).

Therefore, in this phase, four treatments were imposed for 14 days: Fe0, Fe10, VIGS-0, and VIGS-10. At the end, three plants per treatment were analyzed.

2.2 | VIGS assay

The TRV1 and TRV2-*LeFRO1* VIGS vectors were previously described by Gama et al. (2017). Briefly, for TRV2-*LeFRO1* a 303 bp DNA fragment of the *Lycopersicon esculentum* FCR (*FRO1*) sequence (GenBank accession AY224079.1) including bases 1094–1396 and a 29 bp attB recombination sequence were spliced (purchased from Life Technologies). Afterward, the fragment was amplified by polymerase chain reaction (PCR) using Pfu DNA polymerase with the designed primers: forward (5′-GGG GAC AAG TTT GTA CAA AAA AGC AGG CT-3′) and reverse (5′-GGG GAC CAC TTT GTA CAA GAA AGC TGG GT-3′). The resulting PCR product was cloned into the cDNA of TRV2, downstream of the coat protein gene, by the GATEWAY recombination system. The TRV2-*LeFRO1* clone was generated through LR recombination by mobilizing the entry clone containing attL recombination sites to the TRV RNA2 vector (pYL279) having attR recombination sites by using the LR Clonase enzyme and finally transformed into *E. coli* Mach1 chemical competent cells and selected on Luria-Bertani (LB) plates containing Kanamycin (50 μg mL^{-1}).

Concerning the VIGS assay, pTRV1 and pTRV2-*LeFRO1* were introduced into chemically competent *Agrobacterium tumefaciens* strain C58C1 by electroporation and selected on LB plates having Kanamicin, Gentamicin, and Rifampicin, each at 50 μg mL^{-1}. The cultures were grown separately in LB medium containing 10 mM MES buffer, 20 μM acetosyringone, and the respective antibiotics at 28°C in an orbital shaker until an optical density at 600 nm (OD) of 0.6 was attained. The cultures were then harvested and resuspended in infiltration medium (10 mM $MgCl_2$, 10 mM MES, and 100 μM acetosyringone), with a pH adjusted to 5.6. pTRV1 and pTRV2-*LeFRO1* cultures were mixed in a 1:1 ratio and left at room temperature for approximately 3 h. The inoculation of the vectors was carried out by agroinfiltration, using a 1 mL needleless syringe on the abaxial side of all leaves of the selected plants (30 plants).

2.3 | Detection of the TRV vector

Detection of the TRV vector was performed in newly developed leaves after inoculation with the VIGS vector. The detection was done by double antibody sandwich-enzyme linked immune sorbent assay (DAS-ELISA) using specific commercial antibodies against TRV (Sediag, INRA), and the protocol was followed as indicated by the manufacturer. Only 25 plants, all TRV-positive in the DAS-ELISA test, were selected and used for the experiment.

TRV–green fluorescent protein (GFP) was inoculated to a set of plants of Fe0.5 and used as a control to evaluate the effect of the vector per se. As the GFP does not have any homology to plant DNA it will not cause silencing. Visual detections of control plants with GFP fluorescence expression were observed in whole plants under a 100 W handheld long wavelength ultraviolet lamp (Black Ray model B 100AP, UV products) and photographed with a Cannon digital camera (Canon EOS 450D). As an example, in Figure 2 green fluorescence was observed in young leaves of an inoculated plants. The inoculation was done in older leaves of this plant, supporting the efficacy of inoculation procedure.

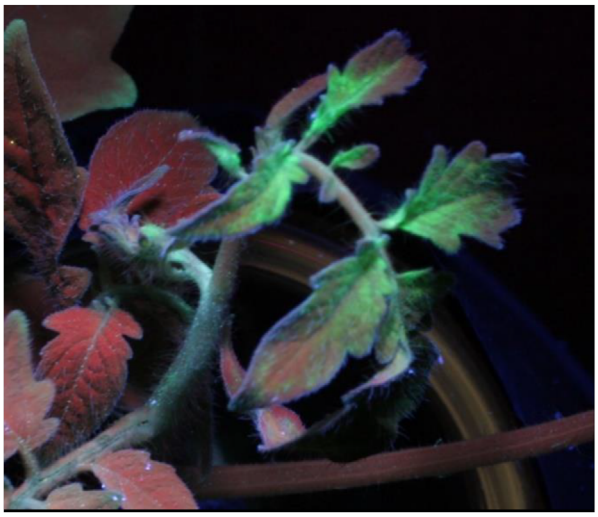

FIGURE 2 Validation of the tobacco rattle virus–green fluorescent protein (TRV–GFP) infiltrated vector in Fe0.5 plants. Plants (detail of young leaves) were photographed under a UV-lamp at the end of phase I.

2.4 | Total leaf chlorophyll concentration and SPAD determinations

Leaf chlorophyll (Chl) was estimated nondestructively using a portable SPAD-502 apparatus (Minolta Corp). During the experimental period, SPAD values were taken in young fully developed leaves of at least three plants per treatment and converted to leaf Chl concentrations. To convert SPAD values into total Chl concentration per unit of leaf area (μmol m^{-2}) of tomato plants from cv. "Cherry," a calibration curve was obtained in a preliminary experiment using plants with different degrees of chlorosis, such as described previously for strawberry plants (Pestana et al., 2011). Briefly, foliar discs with 1 cm of diameter were collected from different leaves and the SPAD values were recorded in each foliar disc. Then, photosynthetic pigments were extracted with 100% acetone in the presence of sodium ascorbate as described by Abadía and Abadía (1993). Total Chl concentration was spectrophotometrically quantified using the protocol reported by Lichtenthaler (1987). The best-adjusted model between SPAD values and total leaf Chl concentration was a quadratic regression model:

$$\text{Chl}\ \left(\mu\text{mol m}^{-2}\right) = 0.157 \times \text{SPAD}^2 + 18.674 \times \text{SPAD} \qquad (1)$$

A strong relationship between SPAD readings and leaf Chl was obtained: $R^2 = 0.95$ at a significant level $p < 0.001$ ($n = 35$).

2.5 | Ferric-chelate reductase (FCR) activity

The activity of the root FCR (EC.1.16.1.17) was measured at the end of each phase (after 26 days—phase I, plus 14 days—phase II) in all plants, using bathophenanthroline disulfonate (BPDS), which forms a red Fe_3BPDS_2 complex with Fe(II), following the methodology reported by Bienfait et al. (1983). Each single root-tip with approximately 2 cm in length (8.4 ± 0.2 mg) excised with a razor blade was incubated in an Eppendorf tube in the darkness for 1 h, with 900 μL of micronutrient-free half-strength Hoagland's nutrient solution, 300 μM BPDS, 500 μM Fe(III)-EDTA and 5 mM MES-KOH, pH 6.0. The FCR activity was then measured at 535 nm, using a spectrophotometer (CADAS 100 UV–VIS photometer; Dr. Lange). Root tips were then blotted on paper and fresh weight (FW) was determined. Values shown for FCR activity were the mean of at least five root tips per plant and three plants were selected in each treatment. A molar extinction coefficient of 22.14 mM^{-1} cm^{-1} was used to convert absorbance values into root Fe reduction rates on a FW basis. Blank controls without root tips were used to correct for any nonspecific photoreduction.

2.6 | Biomass and leaf mineral analysis

At the end of the phase I (Fe0.5 and VIGS-0.5 treatments) and phase II (Fe0, Fe10, VIGS-0, and VIGS-10 treatments), three plants from each treatment were collected and separated into roots, stems, mature leaves, and young leaves.

The plant material was washed to remove any contamination, first with tap water, followed by deionized water with a nonionic detergent, and then with 0.01 M HCl. Finally, three rinses were made with distilled water. FW was determined for each collected sample which was dried at 60°C until constant weight to record dry weight (DW). Samples were then grounded to a powder and ashed at 450°C, followed by digestion with 1 M HCl. Phosphorus was determined colorimetrically by the molybdovanadate method. Potassium was determined by emission spectrophotometry and Ca, Mg, Mn, Zn, Cu, and Fe were determined by atomic absorption spectrophotometry (SolaarM Series, Pye Unicam) following standard methods (AOAC, 1990). Nutrient partitioning by plant organ was determined based on the values of nutrients contents, which were calculated using the concentration and the respective DW values. The Fe uptake rate (μg Fe day^{-1}) per organ was calculated for each plant at day 26 (phase I). At day 40 (phase II) this rate was calculated as the difference between the Fe content in plants grown with 10 μM of Fe (Fe10 plants in phase II) and with 0.5 μM of Fe (Fe0.5 plants in phase I). The same procedure was also done to silenced plants (VIGS-10 and VIGS-0.5 plants).

2.7 | RNA isolation and qRT-PCR analysis

At the end of phase I, total RNA was extracted from root tips for both treatments, Fe0.5 and VIGS-0.5. For this analysis, a composite sample of three biological replicates for each treatment was used. Approximately 100 mg of plant FW was used for RNA extraction with guanidinium thiocyanate-phenol-chloroform extraction (TRIzol Reagent, Ambion) according to the manufacturer's guide. RNA extractions were cleaned up with Turbo DNA-free Kit (Applied Biosystems) according to manufacturer's instructions. The quality and concentration of all the RNA preparations were determined by using a NanoDrop

2000c spectrophotometer (Thermo Scientific). The ratio of absorbance at 260 and 280 nm was used to assess the purity of RNA; in all samples, it was greater than 1.80.

cDNA synthesis and PCR amplification were carried out in one step using iScript one-step reverse transcriptional (RT)-PCR kit with SYBR Green (Bio-Rad). A 101-bp fragment was amplified from *LeFRO1* mRNA with the forward primer: 5′-TTG AGA TTC TTA CAG TCA CGA-3′ and the reverse primer: 5′-CTT AAA CCT TTA GTC TTG GAG-3′ that anneal outside the region targeted for silencing so that only the endogenous gene may be quantified.

The amplifications were carried out on an iCycler iQ (Bio-Rad, USA), and the mixtures were prepared in a final volume of 15 μL containing 7.3 μL of 2× SYBR Green master mix, 0.3 μL (4 nM) of each amplification primers, 0.3 μL of iScript reverse transcriptase, and 1 μL (20 ng) of the RNA template.

The following thermal cycling conditions were used: reverse transcription for 10 min at 50°C, denaturation for 5 min at 95°C, followed by 40 cycles of 10 s of denaturation at 95°C, 30 s for annealing at 55°C, and 30 s at 72°C for extension.

To quantify gene expression, a calibration curve was generated using a seven-point serial dilution, and a PCR efficiency of 91.3% was obtained for the transcript (Pfaffl, 2001). The relative expression of the gene of interest was calculated based on the efficiency of RT-PCR (E) and the variation of the number of cycles threshold (ΔCT) between the control sample (in this case a control Fe0.5 plants) and of the unknown sample (VIGS-0.5 plants).

$$\text{mRNA FRO1} = (1+E)^{(\Delta CT = CT\text{Fe0.5} - CT\text{VIGS} - 0.5)} \quad (2)$$

For each sample, the relative level of *LeFRO1* mRNA was determined in root tips and normalized taking into consideration the number of secondary root tips counted in each treatment.

2.8 | Statistical analysis

Analysis of variance (F-test) for all treatments was compared using the one-sample t-test or the Duncan multiple range test at $p < 0.05$ (IBM SPSS software, version 20).

3 | RESULTS

3.1 | Leaf chlorophyll (Chl)

During phase I (26 days), Fe0.5 plants remained green, without chlorosis symptoms (Figure 3A). VIGS-0.5 plants clearly developed Fe deficiency symptoms. No visual symptoms of Fe chlorosis were observed in Fe0.5 or TRV–GFP plants.

The leaf Chl concentration was around 702 ± 18 μmol m^{-2}. In contrast, VIGS-0.5 plants showed typical Fe-deficiency symptoms with leaf total Chl concentration consistently decreasing from day 14 until the end of the phase I (310 ± 16 μmol m^{-2}) (Figure 4A).

During the second phase of the experiment, plants grown without Fe (VIGS-0 and Fe0) maintained (VIGS-0) or developed (Fe0) typical symptoms of Fe chlorosis in young leaves (Figure 3B). The level of Chl in these plants decreased until it reached mean values around 135.2 ± 25.9 μmol Chl m^{-2} (Figure 4B). Tomato plants grown under 10 μM of Fe in the nutrient solution remained green over the experimental period. Plants of the Fe10 treatment reached the maximum value of leaf Chl at the end of the phase II (1096.8 ± 59.8 μmol Chl m^{-2}), whereas plants previously inoculated with VIGS (VIGS-10) reached the maximum value earlier, at day 37 (803.1 ± 29.0 μmol Chl m^{-2}; 73% lower than that of Fe10 plants), which then remained similar until the end of the experiment. Nevertheless, during phase II, the increase in units of Chl in VIGS-10 plants was higher (2.1-fold) than in Fe10 plants (1.6-fold).

3.2 | Biomass partitioning

The height, number of leaves, and the total DW of roots, stems, young, and mature leaves at the end of each phase are shown in Table 1.

After 26 days (end of phase I), Fe0.5 plants tended to be taller, with more leaves and greater biomass than VIGS-0.5 plants (Table 1). VIGS-0.5 plants had significantly higher root-to-shoot ratio, indicating a greater investment in root biomass under Fe deficiency.

Plants accumulated most of their biomass during phase II, so that on average it was 2.2 times (silenced plants) to 3.5 times (controls) greater than at the end of phase I. The addition of a higher level of Fe to the nutrient solution resulted in a greater height and number of leaves, and a smaller root/shoot ratio in Fe10 compared with Fe0 plants. In contrast, in silenced plants (VIGS-0 and VIGS-10), the addition of more Fe was not translated into different growth parameters between both treatments 14 days later (day 40).

3.3 | Root FCR activity and expression of the *FRO1* gene

Regardless of the phase, silenced plants (VIGS-0.5 plants in phase I, and VIGS-0 and VIGS-10 in phase II) presented smaller roots with subapical root swelling, typical of Fe deficiency (Figure 3C). Additionally, young lateral roots from chlorotic plants showed a subapical swelling zone densely covered with short root hair. These changes were not observed in the other treatments, including in plants of the TRV–GFP treatment at the end of phase I.

At day 26 (Figure 5A), VIGS-0.5 plants had lowered *LeFRO1* mRNA expression values (0.57) compared to control Fe0.5 plants (0.78). Additionally, root FCR activity was significantly lower in silenced plants (VIGS-0.5: 26 ± 2 nmol Fe(II) min^{-1} g^{-1} FW) than in control plants (Fe0.5: 31 ± 1 nmol Fe(II) min^{-1} g^{-1} FW). In agreement, the root tips of the silenced plants (VIGS-0.5) did not show the typical pink coloration indicating the absence of Fe reduction as observed in the root tips of the control plants (Fe0.5).

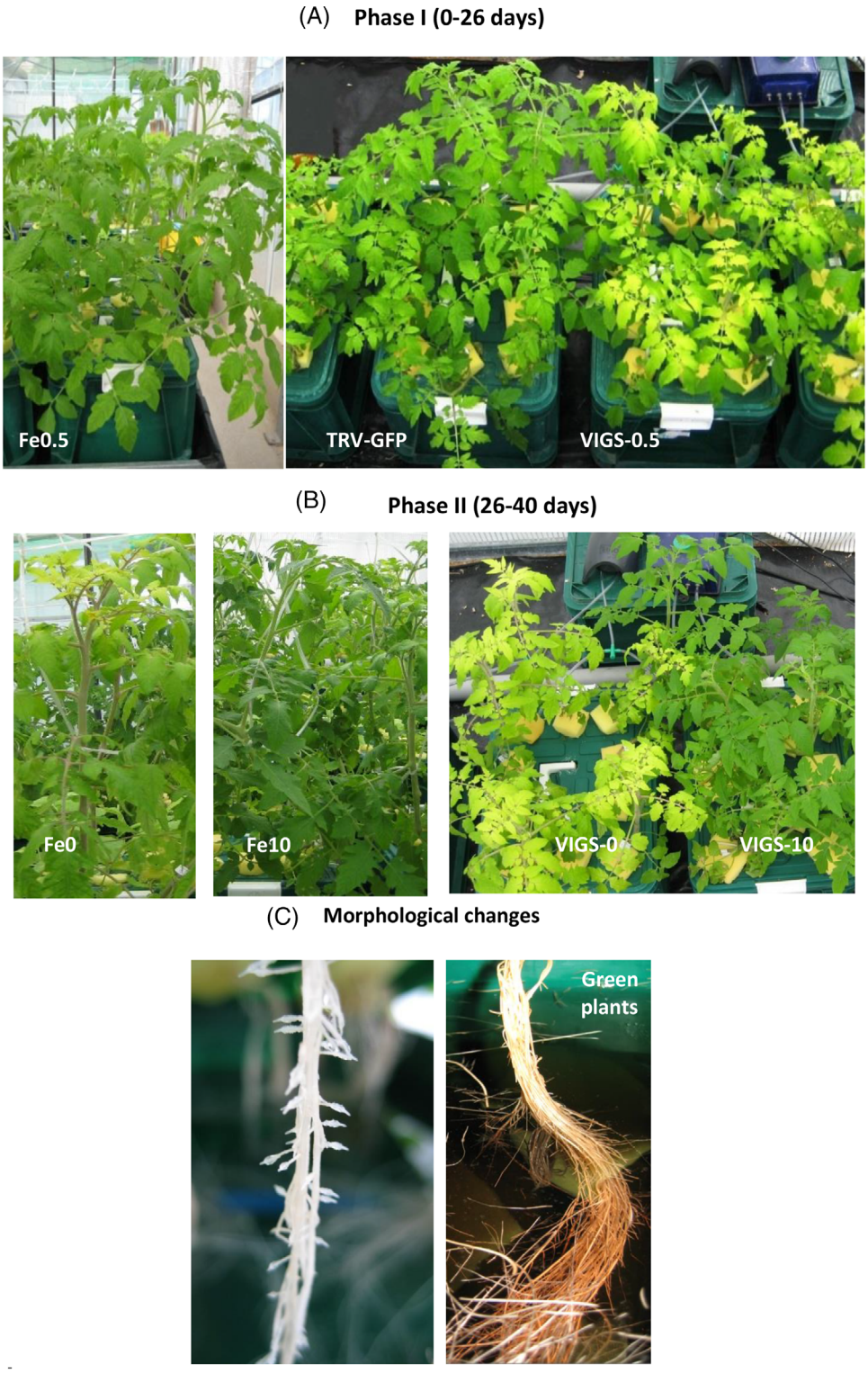

FIGURE 3 Aspect of tomato cv. "Cherry" plants at the end of the phase I (day 26) and at the end of the phase II (day 40). (A) Phase I—treatments are Fe0.5 (control plants; 0.5 μM of Fe) and virus-induced gene silencing (VIGS)-0.5 (silenced plants; 0.5 μM of Fe). Vector control plants (tobacco rattle virus–green fluorescent protein [TRV–GFP]) are also shown. (B) Phase II—treatments are Fe0 (no iron), Fe10 (10 μM of Fe), VIGS-0 (silenced plants; no iron), and VIGS-10 (silenced plants; 10 μM of Fe). (C) Roots of chlorotic and green plants.

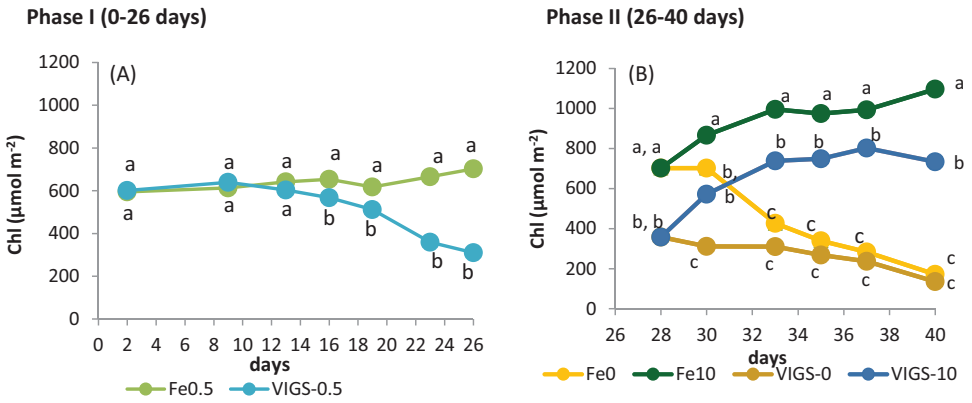

FIGURE 4 Total chlorophyll (Chl) concentration (µmol m^{-2}) in young leaves of plants of different treatments during the experimental period. (A) Phase I—treatments are Fe0.5 (control plants; 0.5 µM of Fe) and virus-induced gene silencing (VIGS)-0.5 (silenced plants; 0.5 µM of Fe). (B) Phase II—treatments are Fe0 (no iron), Fe10 (10 µM of Fe), VIGS-0 (silenced plants; no iron), and VIGS-10 (silenced plants; 10 µM of Fe). Phase I: $n = 5$ and phase II: $n = 3$. For each phase, means with different letters were significantly different at $p < 0.05$, using the *F*-test (phase I) and the Duncan multiple range test (phase II).

TABLE 1 Effect of treatments on number of leaves, plant height, dry weight of roots, stem, mature leaves and young leaves, and biomass partition between root and shoot of tomato plants.

			Dry weight (g)					
	Plant height (cm)	Number of leaves	Roots	Stems	Mature leaves	Young leaves	Total plant	Root/shoot (DW)
Phase I—(26 days)								
Fe0.5	48.4 ± 1.1 a	11.0 ± 0.4 a	0.17 ± 0.11 a	0.66 ± 0.47 a	0.80 ± 0.15 a	0.43 ± 0.15 a	2.06 ± 0.22 a	0.12 ± 0.01 b
VIGS-0.5	23.1 ± 0.8 b	9.3 ± 0.3 b	0.12 ± 0.04 b	0.23 ± 0.03 b	0.22 ± 0.09 b	0.20 ± 0.06 b	0.77 ± 0.06 b	0.17 ± 0.01 a
Phase II—(40 days)								
Fe0	58.2 ± 8.2 b	15.2 ± 2.2 b	0.70 ± 0.10 a	2.30 ± 0.65 a	1.57 ± 0.67 ab	1.57 ± 0.03 b	6.14 ± 0.36 a	0.14 ± 0.03 a
Fe10	78.2 ± 6.0 a	23.6 ± 3.4 a	0.77 ± 0.24 a	2.60 ± 0.56 a	2.27 ± 1.01 a	2.17 ± 0.37 a	7.81 ± 0.55 a	0.10 ± 0.01 b
VIGS-0	28.2 ± 3.2 c	9.8 ± 0.7 ab	0.16 ± 0.03 b	0.70 ± 0.10 b	0.43 ± 0.03 b	0.37 ± 0.07 c	1.66 ± 0.06 b	0.10 ± 0.01 b
VIGS-10	38.5 ± 1.2 c	19.8 ± 2.7 ab	0.21 ± 0.10 b	0.67 ± 0.10 b	0.43 ± 0.12 b	0.47 ± 0.09 c	1.78 ± 0.10 b	0.12 ± 0.11 b

Note: The means were presented at the end of the two phases of the experiment: phase I—after 26 days of the beginning and treatments are Fe0.5 (control plants; 0.5 µM of Fe) and VIGS-0.5 (silenced plants; 0.5 µM of Fe); and phase II—after 14 days and treatments are Fe0 (no iron), Fe10 (10 µM of Fe), VIGS-0 (silenced plants; no iron), and VIGS-10 (silenced plants; 10 µM of Fe). Phase I: $n = 5$ and phase II: $n = 3$. For each phase, means with different letters were significantly different at $p < 0.05$, using the *F*-test (phase I) and the Duncan multiple range test (phase II).
Abbreviations: DW, dry weight; VIGS, virus-induced gene silencing.

At the end the experiment (40 days; Figure 5B), values of root FCR activity in roots tips were considerably lower than those observed at day 26 in all treatments. FCR activity measured was significantly higher in VIGS-10 plants (12.9 ± 1.8 nmol Fe(II) min^{-1} g^{-1} FW) than in the Fe10 or VIGS-0 plants (5.4 ± 0.9 and 6.3 ± 1.1 nmol Fe(II) min^{-1} g^{-1} FW, respectively).

3.4 | Nutrients concentration and partitioning

The effects of treatments on the concentration of macronutrients are shown in Table 2. In phase I, silenced plants (VIGS-0.5) had higher P and Mg concentrations in all plant organs than control plants (Fe0.5). However, the total content in silenced plants was only 28% (P) and 22% (Mg) of that of control, and there were no significant differences in nutrient allocation between plant organs (Figure 6). In phase II, P concentration tended to continue higher in silenced plants (not significantly different in roots).

After 26 days, there was a tendency for higher concentrations of Ca in aboveground tissues of silenced plants, although a significant difference was only found for Ca in stems. In contrast, K concentration tended to be lower in VIGS-0.5 plants, although only significantly different in stems and mature leaves. Once again total plant content in silenced plants was only about 20% (Ca) and 14% (K) of that of controls.

At the end of phase II, K concentration decreased in roots when Fe was supplied and increased in stems. Magnesium concentrations

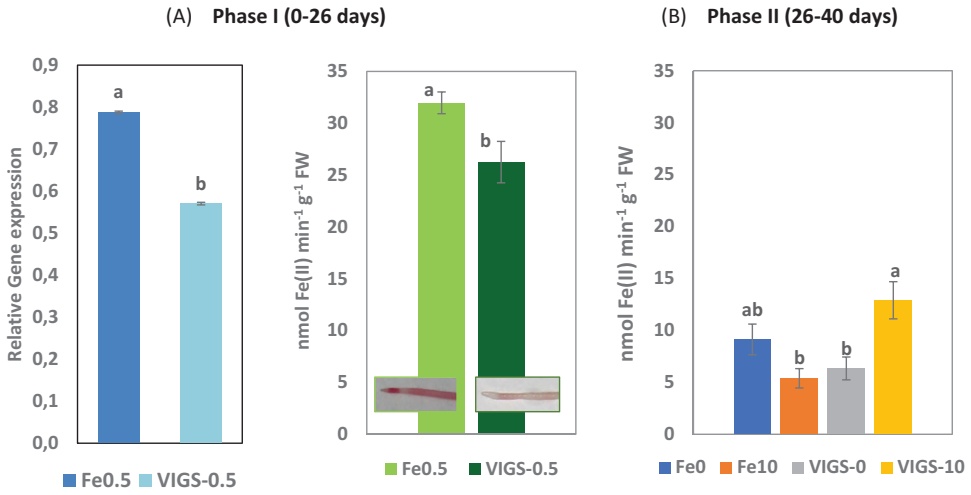

FIGURE 5 LeFRO1 relative expression and ferric-chelate reductase (FCR) activity (nmol Fe(II) min^{-1} g^{-1} fresh weight [FW]) evaluated in root tips at day 26. (A) Phase I—treatments are Fe0.5 (control plants; 0.5 μM of Fe) and virus-induced gene silencing (VIGS)-0.5 (silenced plants; 0.5 μM of Fe), and at day 40. (B) Phase II—treatments are Fe0 (no iron), Fe10 (10 μM of Fe), VIGS-0 (silenced plants; no iron), and VIGS-10 (silenced plants; 10 μM of Fe). Phase I: $n = 5$ and phase II: $n = 3$. For each phase, means with different letters were significantly different at $p < 0.05$, using the *F*-test or the one-sample *t*-test (phase I), and the Duncan multiple range test (phase II). Photographs of root tips are shown on the graph.

in roots were not affected by treatments. In stems, the highest value of Mg concentration was registered in VIGS-10 plants although only significantly different from Fe10 plants. In treatment VIGS-0, Mg concentration was significantly higher in young and mature leaves compared to the other treatments. Regarding Ca in roots and in young leaves, no significant differences were found between treatments. Silenced plants (VIGS-0 and VIGS-10) showed the highest values of Ca in mature leaves and in the case of stems, VIGS-10 had the highest concentration.

The effects of treatments on the concentration and allocation of micronutrients are shown in Table 3 and Figure 7.

At the end of phase I, the concentrations of all micronutrients studied were higher in silenced plants, although not necessarily in all organs. This was true for roots (Cu), all organs (Zn), stems and leaves (Mn), and roots and stems (Fe). The total content of micronutrients was less affected by silencing than were macronutrients. In fact, although Fe content in silenced plants was the most impaired of micronutrients, it was still 31% of control, whereas Cu and Mn were reduced to 45% and Zn to just 75% of the content in control plants. In these plants, the allocation of Cu and Zn to roots increased at the expense of stems (Cu) or young leaves (Zn). In contrast, less Mn was allocated to roots in silenced plants, but rather to leaves. Less Fe was allocated to leaves in silenced plants.

At the end of phase II, the concentrations of micronutrients continued to be higher in silenced plants. The spike with a high level of Fe in the nutrient solution resulted in a few changes: the concentrations of both Zn and Mn in VIGS-10 plants tended to increase in stems and decrease in young leaves compared with VIGS-0 plants. The total content of Cu was higher in silenced plants grown with Fe (90 μg per plant) compared with VIGS-0 (40 μg per plant), with no significant differences for Zn or Mn. In silenced plants, there was a major change in the allocation pattern with Cu in roots decreasing to less than 10% of total Cu in VIGS-10 plants compared with 40% of total in VIGS-0 plants.

The concentration of Fe increased in all organs in the VIGS-10 treatment compared to other treatments with or without Fe in the solution, but the allocation pattern remained similar to VIGS-0 plants.

Iron uptake rate in each organ is shown in Table 4. During phase I, the uptake rate was higher in control plants, although much smaller than during phase II, presumably as a consequence of small plant size. During phase II, silenced and non-silenced plants showed similar values of Fe uptake rate in roots and mature leaves (10.2 and 3.9 μg Fe day^{-1}, respectively). However, silenced plants had iron uptake rates of 63% and 50% in young leaves and stems, respectively, compared to control plants. Similarly, Fe uptake rate per plant (including all organs assessed) decreased 33% in silenced plants compared to control plants.

4 | DISCUSSIONS

Tomato plants are susceptible to Fe deficiency and develop a series of adaptive physiological and morphological traits (reviewed by Abadía et al., 2011). In the present experiment, the response to Fe deficiency of silenced tomato plants at root level which started with the emission of young lateral roots, followed by root swelling, are in accordance with previous results (Jiménez González et al., 2019). Simultaneously, the decline of leaf chlorophyll concentration and increased root/shoot ratio in silenced plants were also in line with the results previously reported in other species (Pestana et al., 2011, 2012). Silenced plants also displayed lower root FCR activity and a lower root *LeFRO1* mRNA expression value suggesting that agroinoculation with the TRV-*LeFRO1* VIGS vector obstructed the reduction of Fe(III) to Fe(II) at the root surface.

TABLE 2 Macronutrient concentrations (in mg g^{-1} dry weight [DW]) in different plant organs at the end of each phase.

		P	K	Mg	Ca
(mg g^{-1} DW)					
Phase I—(0–26 days)					
Roots	**Fe0.5**	9.4 ± 0.8 b	46.8 ± 2.3 a	6.9 ± 0.5 b	10.2 ± 0.3 a
	VIGS-0.5	11.9 ± 0.5 a	38.0 ± 4.5 a	8.8 ± 0.2 a	12.0 ± 1.2 a
Stems	**Fe0.5**	5.3 ± 0.3 b	120.4 ± 4.3 a	7.2 ± 0.7 b	16.1 ± 0.7 b
	VIGS-0.5	8.4 ± 0.6 a	96.1 ± 1.7 b	8.5 ± 0.2 a	22.1 ± 0.5 a
Mature leaves	**Fe0.5**	5.8 ± 0.3 b	64.9 ± 2.3 a	9.6 ± 0.7 b	47.5 ± 0.3 a
	VIGS-0.5	9.0 ± 0.9 a	46.5 ± 7.3 b	13.9 ± 0.7 a	68.1 ± 6.9 a
Young leaves	**Fe0.5**	8.0 ± 0.3 b	58.2 ± 4.7 a	6.9 ± 0.5 b	27.5 ± 3.1 a
	VIGS-0.5	12.8 ± 0.5 a	55.1 ± 1.9 a	8.8 ± 0.6 a	33.8 ± 1.2 a
Phase II—(26–40 days)					
Roots	**Fe0**	5.9 ± 0.4 a	40.9 ± 2.3 ab	5.4 ± 2.0 a	13.0 ± 3.2 a
	Fe10	7.2 ± 2.3 a	27.8 ± 8.7 ab	4.8 ± 2.2 a	15.2 ± 8.0 a
	VIGS-0	5.6 ± 0.1 a	49.6 ± 9.7 a	5.0 ± 1.3 a	9.4 ± 3.5 a
	VIGS-10	5.2 ± 0.8 a	20.1 ± 10.1 b	2.0 ± 0.8 a	12.3 ± 2.5 a
Stems	**Fe0**	5.1 ± 0.5 b	59.4 ± 7.9 c	4.1 ± 1.0 ab	15.7 ± 3.3 ab
	Fe10	3.5 ± 0.2 c	83.0 ± 3.0 ab	3.1 ± 0.7 b	12.4 ± 2.2 b
	VIGS-0	6.6 ± 0.6 a	63.6 ± 2.6 bc	4.2 ± 0.1 ab	16.7 ± 2.1 ab
	VIGS-10	7.1 ± 0.4 a	87.4 ± 10.4 a	6.0 ± 0.1 a	23.6 ± 1.9 a
Mature leaves	**Fe0**	4.6 ± 1.0 c	39.4 ± 3.1 b	6.2 ± 0.3 c	26.3 ± 4.1 c
	Fe10	4.7 ± 0.5 c	61.5 ± 8.1 a	8.1 ± 1.0 bc	42.0 ± 5.7 b
	VIGS-0	7.7 ± 0.5 b	45.4 ± 1.2 ab	13.8 ± 0.3 a	58.2 ± 1.8 a
	VIGS-10	9.9 ± 0.2 a	43.7 ± 6.9 ab	8.9 ± 0.9 b	59.5 ± 5.3 a
Young leaves	**Fe0**	5.1 ± 1.0 b	38.1 ± 2.8 b	5.8 ± 0.5 b	22.3 ± 3.7 a
	Fe10	5.9 ± 0.2 b	52.4 ± 3.4 a	5.8 ± 0.3 b	26.0 ± 1.4 a
	VIGS-0	7.5 ± 1.0 ab	52.7 ± 0.4 a	9.7 ± 0.8 a	29.9 ± 1.3 a
	VIGS-10	8.7 ± 0.6 a	53.5 ± 7.7 a	6.5 ± 0.9 b	37.0 ± 9.2 a

Note: Phase I—day 26: Treatments are Fe0.5 (control plants; 0.5 μM of Fe) and VIGS-0.5 (silenced plants; 0.5 μM of Fe); and phase II—after 14 days and treatments are Fe0 (no iron), Fe10 (10 μM of Fe), VIGS-0 (silenced plants; no iron), and VIGS-10 (silenced plants; 10 μM of Fe). Results are averages ± standard errors. Phase I: $n = 5$ and phase II: $n = 3$. For each phase, means with different letters were significantly different at $p < 0.05$, using the *F*-test (phase I) and the Duncan multiple range test (phase II).
Abbreviation: VIGS, virus-induced gene silencing.

In general, FCR activity was lower in all treatments in phase II compared to phase I, suggesting a time effect that overcame Fe conditions. It is not possible to prove this hypothesis as we did not measure the time-course of the enzyme; however, previous work by Gogorcena et al. (2000) showed that in vivo FCR activity in a peach rootstock changed over time. Besides, other factors like leaf chlorophyll and Fe leaf concentration may also affect the activity of the enzyme (Abadía et al., 2011; Zhao et al., 2020). According to Jiménez González et al. (2019), FCR activity in roots of tomato plants (cv. "Roma") was substantially increased in Fe-deficient conditions. In our experiment, a similar trend was observed at the end of phase II in Fe0 and Fe10 plants, although without significant differences. This result was probably related to the high morphological variability of the roots apexes sampled for analysis. At this date, the root systems of tomato plants were large and dense, which may have impaired a proper sampling of the roots tips. The fact that plants of VIGS-10 had higher FCR activity (which was statistically similar to Fe0 plants) led to the assumption that after 40 days, the silencing effect was no longer effective.

At the beginning of phase II, it was not entirely clear what would be the extension of the residual silencing effect. In *N. benthamiana*, the addition of Fe to silenced plants could not overcome the consequences of the repression of the *FRO1* gene on physiological processes (Gama et al., 2017). In the present experiment, at day 40, silenced tomato plants were still negatively affected as these plants (VIGS-0 and VIGS-10) were still smaller with less biomass in roots, stems, and young leaves compared with control. However, the increase in total Chl concentration and the higher root FCR activity in the VIGS-10 treatment suggest a reboot of the Fe reduction system in the presence of a high

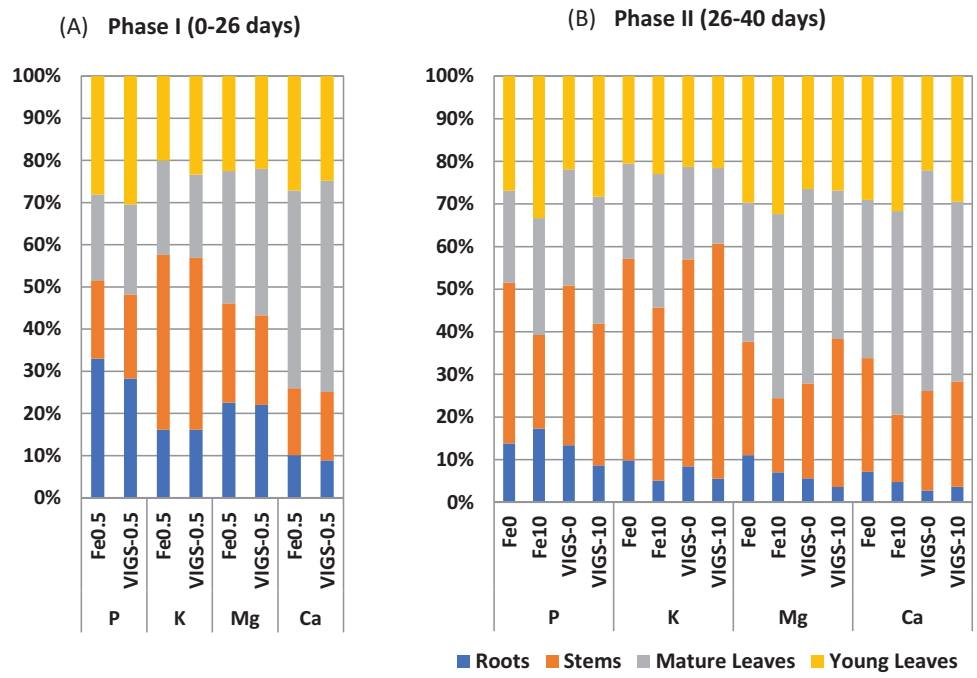

FIGURE 6 Macronutrient partitioning (%) for each nutrient at the end of the experiment. (A) Phase I—day 26: Treatments are Fe0.5 (control plants; 0.5 μM of Fe) and virus-induced gene silencing (VIGS)-0.5 (silenced plants; 0.5 μM of Fe) and (B) phase II—day 40: Fe0 (no iron), Fe10 (10 μM of Fe), VIGS-0 (silenced plants; no iron), and VIGS-10 (silenced plants; 10 μM of Fe). Phase I: $n = 5$ and phase II: $n = 3$.

level of Fe in solution. Regarding Chl, as the silenced plants started phase II with lower values, they were not able to completely overcome this limitation and did not reach the maximum values registered in the plants that always grew with Fe. Thus, silencing of *LeFRO1* seemed less intense in the second phase of the experiment. This may be due to lower titters of virus infection (Ghoshal & Sanfaçon, 2015) or to the induction of a plant mechanism. For example, residual protein concentrations might have been sufficient to carry out their functions without phenotypic alterations leading to an adjustment instead of permanent damage to the photosynthetic apparatus (Gama et al., 2016; López-Millán et al., 2001; Pestana et al., 2012; Velásquez et al., 2009). It has also been described that, depending on the species, effective VIGS tend to decrease after 1 month, that is, that the effect of VIGS seems to be transient (Ratcliff et al., 2001; Ryu et al., 2004; Shi et al., 2021).

Metal homeostasis results from the way plants face deficiency or toxicity of a particular nutrient and is essential to ensure adequate metabolic activity and optimum plant growth (Rai et al., 2021). The understanding of Fe homeostasis in plants has been investigated in recent years and involves all Fe processes, such as trafficking, transporters, storage, and partition in plant organs (Jeong & Guerinot, 2009; Rai et al., 2021). Nonetheless, there is still a need to clarify the key signals that trigger long-distance root-to-shoot responses in Fe-deficient plants. These might explain the upregulation of Fe acquisition genes as a response to Fe chlorosis based on a crosstalk between leaves and roots induced by hormone signals (ethylene and nitric oxide) or by Fe, itself, in the phloem. Furthermore, these signals, local as well as systemic, are believed to be transmitted by a transduction cascade response that leads to enhanced Fe uptake (Divte et al., 2021).

Changes in nutrient homeostasis can be a consequence of nutritional deficiencies, but the effects of silencing one specific gene on nutrients uptake and partitioning are not well-known. Higher concentrations of P and Mg, and to a lesser extend also K, in silenced plants can be attributed to a "concentration effect" since those plants had less biomass at the end of phase I. This pattern was also observed in phase II where P was also higher in stressed silenced plants, as well as Mg in leaves of VIGS-0 plants. The same pattern was not observed for K. Its role as a free osmolyte may explain the absence of differences between silenced and non-silenced plants and the lack of response of K to Fe addition.

The relationship between above and below ground organs maintains the plants as balanced systems in terms of uptake and use (Zhao et al., 2020). Silencing of the *FRO* gene, involved in Fe reduction at root level, was expected to change micronutrients homeostasis, or at least, Fe dynamics. In phase I, it was clear that Cu and Zn were preferentially allocated to roots in silenced plants, but not Mn, which was found mainly in young leaves, probably due to its low mobility in phloem (Rengel, 2001). In phase II, the silencing effect may have been less intense, as already discussed, and plants reorganized the nutritional balance of Cu, Zn, and Mn by allocation to other organs rather than roots. Copper was a special case, since it was very low in roots from phase II, and present mainly in stems. It is probable that this redistribution was partially related to the increase of vegetative growth that occurred in this phase.

The decrease of Fe uptake in silenced plants was apparent in all plant organs during phase I. However, during phase II, the uptake rate was similar in roots and mature leaves, but still lower in stronger sinks

TABLE 3 Micronutrient concentrations (in μg g^{-1} dry weight [DW]) in different plant organs at the end of each phase.

		Cu	Zn	Mn	Fe
(μg g^{-1} DW)					
Phase I—(0–26 days)					
Roots	**Fe0.5**	67.3 ± 4.3 b	102.8 ± 8.6 b	1923.2 ± 63.9 a	128.4 ± 11.4 b
	VIGS-0.5	151.8 ± 2.6 a	541.2 ± 20.4 a	1929.6 ± 263.6 a	227.8 ± 26.3 a
Stems	**Fe0.5**	14.4 ± 1.8 a	36.1 ± 2.5 b	86.1 ± 4.9 b	29.8 ± 7.2 b
	VIGS-0.5	13.8 ± 2.0 a	165.9 ± 13.1 a	236.7 ± 12.7 a	87.1 ± 18.5 a
Mature leaves	**Fe0.5**	16.7 ± 1.6 a	57.4 ± 3.5 b	394.2 ± 24.2 b	75.6 ± 7.0 a
	VIGS-0.5	28.1 ± 15.3 a	154.6 ± 30.4 a	863.4 ± 101.2 a	101.4 ± 15.5 a
Young leaves	**Fe0.5**	17.4 ± 1.4 a	39.7 ± 0.2 b	139.9 ± 24.5 b	84.4 ± 2.9 a
	VIGS-0.5	28.8 ± 6.3 a	77.0 ± 5.0 a	583.1 ± 19.5 a	98.4 ± 27.1 a
Phase II—(0–40 days)					
Roots	**Fe0**	36.5 ± 15.7 b	150.9 ± 15.6 b	938.9 ± 117.2 b	85.5 ± 26.3 c
	Fe10	29.7 ± 10.0 b	122.8 ± 45.4 b	974.8 ± 74.6 b	200.6 ± 61.2 b
	VIGS-0	114.3 ± 33.9 a	392.7 ± 90.7 a	2317.8 ± 472.4 a	150.9 ± 12.2 b
	VIGS-10	52.1 ± 20.7 ab	376.7 ± 15.5 a	2097.9 ± 113.2 a	889.9 ± 80.3 a
Stems	**Fe0**	4.4 ± 1.8 b	43.6 ± 6.5 c	49.1 ± 12.0 c	21.6 ± 5.9 b
	Fe10	4.3 ± 1.0 b	54.5 ± 5.7 c	56.4 ± 3.4 c	32.1 ± 3.3 b
	VIGS-0	12.9 ± 5.3 a	100.6 ± 7.7 b	134.0 ± 16.9 b	38.0 ± 8.4 b
	VIGS-10	30.8 ± 12.4 a	151.5 ± 7.8 a	195.4 ± 15.5 a	62.8 ± 5.7 a
Mature leaves	**Fe0**	10.4 ± 2.6 b	42.6 ± 4.9 b	249.0 ± 19.0 c	43.1 ± 2.4 c
	Fe10	9.5 ± 1.0 b	36.3 ± 1.4 b	188.5 ± 37.1 c	86.1 ± 12.1 b
	VIGS-0	21.4 ± 4.3 a	107.8 ± 1.1 a	1262.2 ± 38.4 a	70.5 ± 3.3 bc
	VIGS-10	22.5 ± 3.2 a	95.1 ± 18.0 a	664.7 ± 122.1 b	181.2 ± 16.4 a
Young leaves	**Fe0**	10.6 ± 1.9 b	42.2 ± 5.1 bc	227.5 ± 41.8 b	44.0 ± 6.7 d
	Fe10	12.4 ± 1.9 b	32.8 ± 1.7 c	109.2 ± 9.6 b	126.5 ± 4.5 b
	VIGS-0	27.8 ± 4.5 a	66.1 ± 5.0 a	607.3 ± 72.8 a	68.1 ± 4.3 c
	VIGS-10	29.6 ± 3.7 a	52.4 ± 3.0 b	290.7 ± 76.8 b	194.9 ± 7.5 a

Note: Phase I—day 26: Treatments are Fe0.5 (control plants; 0.5 μM of Fe) and virus-induced gene silencing (VIGS)-0.5 (silenced plants; 0.5 μM of Fe); and phase II—after 14 days and treatments are Fe0 (no iron), Fe10 (10 μM of Fe), VIGS-0 (silenced plants; no iron), and VIGS-10 (silenced plants; 10 μM of Fe). Results are averages ± standard errors. Phase I: $n = 5$ and phase II: $n = 3$. For each phase, means with different letters were significantly different at $p < 0.05$, using the *F*-test (phase I) and the Duncan multiple range test (phase II).
Abbreviation: VIGS, virus-induced gene silencing.

(stems and young leaves) of silenced plants (VIGS-10) compared with control (Fe10 plants), although a partial recovery of chlorosis symptoms was observed in the former. In a work on nutritional allocation patterns, Zhao et al. (2020) concluded that the changes in nutrients were consistently smaller in the more active organs such as leaves, than in roots. This means that organs with higher metabolic activity are generally able to regulate the internal nutritional balance to ensure a state of relative constancy essential for metabolic activity. In the present experiment, the opposite was observed (although Zhao et al. [2020] did not include Fe in their study).

Fe uptake and translocation within the plant require coordinated expression and proper localization of transcription factors to efficiently regulate Fe homeostasis (Rai et al., 2021). Blocking crucial steps of Fe uptake, primarily at root level, may require the activation of alternative metabolic pathways to maximize resources. It is possible that Cu could be involved in a specific mechanism to compensate for Fe deficiency stress. This is certainly the case for superoxide dismutases where Cu can compensate for lack of iron (Rai et al., 2021).

5 | CONCLUSIONS

In this study, *FRO1* gene-silenced plants had less Chl synthesis and reduced FCR root activity, but after a period of time (40 days), plants partially overcame the silencing effect and recovery took place. Although biomass was negatively affected at this moment, the results of VIGS-10 plants indicated some physiological recovery of the Fe reduction system. Despite this partial recovery, Fe uptake was still

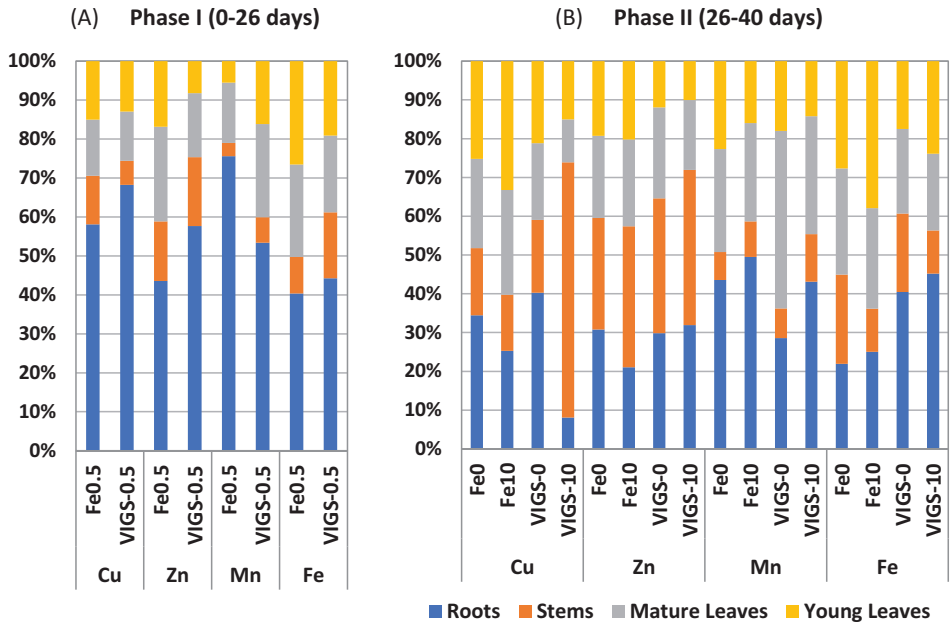

FIGURE 7 Micronutrient partitioning (%) for each nutrient at the end of the experiment. (A) Phase I—day 26: Treatments are Fe0.5 (control plants; 0.5 μM of Fe) and virus-induced gene silencing (VIGS)-0.5 (silenced plants; 0.5 μM of Fe) and (B) phase II—day 40: Fe0 (no iron), Fe10 (10 μM of Fe), VIGS-0 (silenced plants; no iron), and VIGS-10 (silenced plants; 10 μM of Fe). Phase I: $n = 5$ and phase II: $n = 3$.

TABLE 4 Iron uptake rate per organ (μg Fe day^{-1}).

	Phase I		Phase II	
	No VIGS [Fe0.5]	VIGS [VIGS-0.5]	No VIGS [Fe10—Fe0.5]	VIGS [VIGS-10—VIGS-0.5]
Young leaves	1.42	1.17	14.19	5.26
Mature leaves	1.47	0.79	3.86	3.95
Stems	5.14	0.76	2.99	1.55
Roots	2.90	0.65	10.21	10.09
Total	**10.97**	**3.37**	**31.26**	**20.85**

Note: In phase II and for each organ, values were calculated as the difference between the means of Fe contents in Fe10 (10 μM of Fe; phase II) and Fe0.5 (0.5 μM of Fe; phase I) plants, with or without silencing—virus-induced gene silencing (VIGS).
Abbreviation: VIGS, virus-induced gene silencing.

lower in young leaves and in stems of silenced plants. Additionally, Cu and Zn metabolisms were linked to Fe stress conditions, particularly in phase I. Overall, our results suggest that, after initial exposure to stress, silenced tomato plants induce several responses that are not subsequently fully turned off, even after the addition of Fe in the recovery period.

ACKNOWLEDGMENTS

This study was funded by the *National Project* (*PTDC/AGR-PRO/3861/2012*) from *Foundation for Science and Technology* (FCT). T.S. is thankful to FCT for the *Grant SFRH/BD/144764/2019*.

DATA AVAILABILITY STATEMENT

The data that support the findings of this study are available from the corresponding author upon reasonable request.

ORCID

Maribela Pestana https://orcid.org/0000-0002-4319-1682

REFERENCES

Abadía, J., & Abadía, A. (1993). Iron and pigments. In L. L. Barton & B. C. Hemming (Eds.), *Iron chelation in plants and soil microorganisms* (pp. 327–343). Academic Press Inc.

Abadía, J., Vázquez, S., Rellán-Álvarez, R., El-Jendoubi, H., Abadía, A., Álvarez-Fernández, A., & López-Millán, A. F. (2011). Towards a knowledge-based correction of iron chlorosis. *Plant Physiology and Biochemistry*, *49*(5), 471–482.

Agüero, J., del Carmen Vives, M., Velázquez, K., Pina, J. A., Navarro, L., Moreno, P., & Guerri, J. (2014). Effectiveness of gene silencing induced by viral vectors based on Citrus leaf blotch virus is different in *Nicotiana benthamiana* and citrus plants. *Virology*, *460*, 154–164.

AOAC. (1990). *Official methods of analysis* (12th ed.). Springer Nature.

Arce-Rodriguez, M. L., & Ochoa-Alejo, N. (2015). Silencing *AT3* gene reduces the expression of p*Amt*, *BCAT*, *Kas*, and *Acl* genes involved in capsaicinoid biosynthesis in chili pepper fruits. *Biologia Plantarum*, *59*(3), 477–484.

Barberon, M., Dubeaux, G., Kolb, C., Isono, E., Zelazny, E., & Vert, G. (2014). Polarization of Iron-Regulated Transporter 1 (IRT1) to the plant-soil interface plays crucial role in metal homeostasis. *Proceedings of the National Academy of Sciences*, *111*(22), 8293–8298.

Becker, A., & Lange, M. (2010). VIGS-genomics goes functional. *Trends in Plant Science*, *15*(1), 1–4.

Bernal, M., Casero, D., Singh, V., Wilson, G. T., Grande, A., Yang, H., Dodani, S. C., Pellegrini, M., Huijser, P., Connolly, E. L., Mechant, S. S., & Krämer, U. (2012). Transcriptome sequencing identifies *SPL7*-regulated copper acquisition genes *FRO4/FRO5* and the copper dependence of iron homeostasis in *Arabidopsis*. *The Plant Cell*, *24*(2), 738–761.

Bienfait, H. F., Bino, R. J., Van der Bliek, A. M., Duivenvoorden, J. F., & Fontaine, J. M. (1983). Characterization of ferric reducing activity in roots of Fe-deficient *Phaseolus vulgaris*. *Physiologia Plantarum*, *59*(2), 196–202.

Brigneti, G., Martín-Hernández, A. M., Jin, H., Chen, J., Baulcombe, D. C., Baker, B., & Jones, J. D. (2004). Virus-induced gene silencing in *Solanum* species. *The Plant Journal*, *39*(2), 264–272.

Burch-Smith, T. M., Anderson, J. C., Martin, G. B., & Dinesh-Kumar, S. P. (2004). Applications and advantages of virus-induced gene silencing for gene function studies in plants. *The Plant Journal*, *39*(5), 734–746.

Chai, Y. M., Jia, H. F., Li, C. L., Dong, Q. H., & Shen, Y. Y. (2011). FaPYR1 is involved in strawberry fruit ripening. *Journal of Experimental Botany*, *62*(14), 5079–5089.

Connolly, E. L., Campbell, N. H., Grotz, N., Prichard, C. L., & Guerinot, M. L. (2003). Overexpression of the FRO2 ferric chelate reductase confers tolerance to growth on low iron and uncovers posttranscriptional control. *Plant Physiology*, *133*(3), 1102–1110.

Divte, P. R., Yadav, P., Pawar, A. B., Sharma, V., Anand, A., Pandey, R., & Singh, B. (2021). Crop response to iron deficiency is guided by cross-talk between phytohormones and their regulation of the root system architecture. *Agricultural Research*, *10*, 347–360.

Du, J., Huang, Z., Wang, B., Sun, H., Chen, C., Ling, H. Q., & Wu, H. (2015). SlbHLH068 interacts with FER to regulate the iron-deficiency response in tomato. *Annals of Botany*, *116*(1), 23–34.

Fu, D. Q., Meng, L. H., Zhu, B. Z., Zhu, H. L., Yan, H. X., & Luo, Y. B. (2016). Silencing of the *SlNAP7* gene influences plastid development and lycopene accumulation in tomato. *Scientific Reports*, *6*(1), 38664.

Gama, F., Saavedra, T., Da Silva, J. P., Miguel, M. G., de Varennes, A., Correia, P. J., & Pestana, M. (2016). The memory of iron stress in strawberry plants. *Plant Physiology and Biochemistry*, *104*, 36–44.

Gama, F., Saavedra, T., Dandlen, S., de Varennes, A., Correia, P. J., Pestana, M., & Nolasco, G. (2017). Silencing of the *FRO1* gene and its effects on iron partition in *Nicotiana benthamiana*. *Plant Physiology and Biochemistry*, *114*, 111–118.

Ghoshal, B., & Sanfaçon, H. (2015). Symptom recovery in virus-infected plants: Revisiting the role of RNA silencing mechanisms. *Virology*, *479*, 167–179.

Gogorcena, Y., Abadía, J., & Abadía, A. (2000). Induction of in vivo root ferric chelate reductase activity in fruit tree rootstock. *Journal of Plant Nutrition*, *23*(1), 9–21.

Graziano, M., & Lamattina, L. (2007). Nitric oxide accumulation is required for molecular and physiological responses to iron deficiency in tomato roots. *The Plant Journal*, *52*(5), 949–960.

Grotz, N., & Guerinot, M. L. (2006). Molecular aspects of Cu, Fe and Zn homeostasis in plants. *Biochimica et Biophysica Acta (BBA)—Molecular Cell Research*, *1763*(7), 595–608.

He, X., Jin, C., Li, G., You, G., Zhou, X., & Zheng, S. (2008). Use of the modified viral satellite DNA vector to silence mineral nutrition-related genes in plants: Silencing of the tomato ferric chelate reductase gene, *FRO1*, as an example. *Science in China Series C: Life Sciences*, *51*(5), 402–409.

Ivanov, R., Brumbarova, T., & Bauer, P. (2012). Fitting into the harsh reality: Regulation of iron-deficiency responses in dicotyledonous plants. *Molecular Plant*, *5*(1), 27–42.

Jain, A., Wilson, G. T., & Connolly, E. L. (2014). The diverse roles of FRO family metalloreductases in iron and copper homeostasis. *Frontiers in Plant Science*, *5*, 100. https://doi.org/10.3389/fpls.2014.00100

Jeong, J., & Connolly, E. L. (2009). Iron uptake mechanisms in plants: Functions of the FRO family of ferric reductases. *Plant Science*, *176*(6), 709–714.

Jeong, J., & Guerinot, M. L. (2009). Homing in on iron homeostasis in plants. *Trends in Plant Science*, *14*(5), 280–285.

Jiménez González, M. R., Casanova Lerma, L., Saavedra, T., Gama, F., Suárez García, M. P., Correia, P. J., & Pestana, M. (2019). Responses of tomato (*Solanum lycopersicum* L.) plants to iron deficiency in the root zone. *Folia Horticulturae*, *31*(1), 223–234.

Kobayashi, T., & Nishizawa, N. K. (2012). Iron uptake, translocation, and regulation in higher plants. *Annual Review of Plant Biology*, *63*, 131–152.

Lange, M., Yellina, A. L., Orashakova, S., & Becker, A. (2013). Virus-induced gene silencing (VIGS) in plants: An overview of target species and the virus-derived vector systems. In A. Becker (Ed.), *Virus-induced gene silencing. Methods in molecular biology* (Vol. 975, pp. 1–14). Humana Press.

Li, L., Ye, L., Kong, Q., & Shou, H. (2019). A vacuolar membrane ferric-chelate reductase, OsFRO1, alleviates Fe toxicity in rice (*Oryza sativa* L.). *Frontiers in Plant Science*, *10*, 700.

Lichtenthaler, H. K. (1987). Chlorophylls and carotenoids: Pigments of photosynthetic biomembranes. *Methods in Enzymology*, *148*, 350–382.

López-Millán, A. F., Morales, F., Gogorcena, Y., Abadía, A., & Abadía, J. (2001). Iron resupply-mediated deactivation of Fe-deficiency stress responses in roots of sugar beet. *Functional Plant Biology*, *28*(3), 171–180.

Lu, R., Martin-Hernandez, A. M., Peart, J. R., Malcuit, I., & Baulcombe, D. C. (2003). Virus-induced gene silencing in plants. *Methods*, *30*(4), 296–303.

Marschner, H., Römheld, V., & Kissel, M. (1986). Different strategies in higher plants in mobilization and uptake of iron. *Journal of Plant Nutrition*, *9*(3–7), 695–713.

Mukherjee, I., Campbell, N. H., Ash, J. S., & Connolly, E. L. (2006). Expression profiling of the Arabidopsis ferric chelate reductase (*FRO*) gene family reveals differential regulation by iron and copper. *Planta*, *223*, 1178–1190.

Murgia, I., Marzorati, F., Vigani, G., & Morandini, P. (2022). Plant iron nutrition: The long road from soil to seeds. *Journal of Experimental Botany*, *73*(6), 1809–1824.

Pfaffl, M. W. (2001). A new mathematical model for relative quantification in real-time RT–PCR. *Nucleic Acids Research*, *29*(9), e45–e45. https://doi.org/10.1093/nar/29.9.e45

Pestana, M., Correia, P. J., David, M., Abadía, A., Abadía, J., & de Varennes, A. (2011). Response of five citrus rootstocks to iron deficiency. *Journal of Plant Nutrition and Soil Science*, *174*(5), 837–846.

Pestana, M., Correia, P. J., Saavedra, T., Gama, F., Abadía, A., & de Varennes, A. (2012). Development and recovery of iron deficiency by iron resupply to roots or leaves of strawberry plants. *Plant Physiology and Biochemistry*, *53*, 1–5.

Nozoye, T., Aung, M. S., Masuda, H., Nakanishi, H., & Nishizawa, N. K. (2017). Bioenergy grass [*Erianthus ravennae* (L.) Beauv.] secretes two members of mugineic acid family phytosiderophores which involved in their tolerance to Fe deficiency. *Soil Science and Plant Nutrition*, *63*(6), 543–552.

Rai, S., Singh, P. K., Mankotia, S., Swain, J., & Satbhai, S. B. (2021). Iron homeostasis in plants and its crosstalk with copper, zinc, and manganese. *Plant Stress*, *1*, 100008. https://doi.org/10.1016/j.stress.2021.100008

Rajniak, J., Giehl, R. F., Chang, E., Murgia, I., von Wirén, N., & Sattely, E. S. (2018). Biosynthesis of redox-active metabolites in response to iron deficiency in plants. *Nature Chemical Biology*, *14*(5), 442–450.

Ratcliff, F., Martin-Hernandez, A. M., & Baulcombe, D. C. (2001). Technical advance: Tobacco rattle virus as a vector for analysis of gene function by silencing. *The Plant Journal*, *25*(2), 237–245.

Rengel, Z. (2001). Xylem and phloem transport of micronutrients. In W. J. Horst, M. K. Schenk, A. Bürkert, N. Claasen, H. Flessa, W. B. Frommer, H. Goldbach, H.-W. Olfs, V. Römheld, B. Sattelmacher, U. Schmidhalter, S. Schubert, N. von Wirén, & L. Wittenmayer (Eds.), *Plant nutrition. Developments in plant and soil sciences* (pp. 628–629). Springer.

Ricachenevsky, F. K., & Sperotto, R. A. (2014). There and back again, or always there? The evolution of rice combined strategy for Fe uptake. *Frontiers in Plant Science*, *5*, 189. https://doi.org/10.3389/fpls.2014.00189

Ryu, C. M., Anand, A., Kang, L., & Mysore, K. S. (2004). Agrodrench: A novel and effective agroinoculation method for virus-induced gene silencing in roots and diverse *Solanaceous* species. *The Plant Journal*, *40*(2), 322–331.

Robinson, N. J., Procter, C. M., Connolly, E. L., & Guerinot, M. L. (1999). A ferric-chelate reductase for iron uptake from soils. *Nature*, *397*(6721), 694–697.

Sahu, P. P., Puranik, S., Khan, M., & Prasad, M. (2012). Recent advances in tomato functional genomics: Utilization of VIGS. *Protoplasma*, *249*, 1017–1027.

Schmid, N. B., Giehl, R. F., Döll, S., Mock, H. P., Strehmel, N., Scheel, D., Kong, S., Hider, R. C., & von Wirén, N. (2014). Feruloyl-CoA 6′-hydroxylase1-dependent coumarins mediate iron acquisition from alkaline substrates in Arabidopsis. *Plant Physiology*, *164*(1), 160–172.

Senthil-Kumar, M., Gowda, H. R., Hema, R., Mysore, K. S., & Udayakumar, M. (2008). Virus-induced gene silencing and its application in characterizing genes involved in water-deficit-stress tolerance. *Journal of Plant Physiology*, *165*(13), 1404–1421.

Senthil-Kumar, M., & Mysore, K. S. (2011). New dimensions for VIGS in plant functional genomics. *Trends in Plant Science*, *16*(12), 656–665.

Shi, G., Hao, M., Tian, B., Cao, G., Wei, F., & Xie, Z. (2021). A methodological advance of tobacco rattle virus-induced gene silencing for functional genomics in plants. *Frontiers in Plant Science*, *12*, 671091. https://doi.org/10.3389/fpls.2021.671091

Singh, B., Kukreja, S., Salaria, N., Thakur, K., Gautam, S., Taunk, J., & Goutam, U. (2019). VIGS: A flexible tool for the study of functional genomics of plants under abiotic stresses. *Journal of Crop Improvement*, *33*(5), 567–604.

Singh, A. K., Ghosh, D., & Chakraborty, S. (2022). Optimization of tobacco rattle virus (TRV)-based virus-induced gene silencing (VIGS) in tomato. In K. S. Mysore & M. Senthil-Kumar (Eds.), *Plant gene silencing. Methods in molecular biology* (Vol. 2408, pp. 133–145). Humana.

Tian, S. L., Li, L., Chai, W. G., Shah, S. N. M., & Gong, Z. H. (2014). Effects of silencing key genes in the capsanthin biosynthetic pathway on fruit color of detached pepper fruits. *BMC Plant Biology*, *14*(1), 1–12.

Velásquez, A. C., Chakravarthy, S., & Martin, G. B. (2009). Virus-induced gene silencing (VIGS) in *Nicotiana benthamiana* and tomato. JoVE (Journal of Visualized Experiments), *28*, e1292. https://doi.org/10.3791/1292

Vigani, G., Di Silvestre, D., Agresta, A. M., Donnini, S., Mauri, P., Gehl, C., Bittner, F., & Murgia, I. (2017). Molybdenum and iron mutually impact their homeostasis in cucumber (*Cucumis sativus*) plants. *New Phytologist*, *213*(3), 1222–1241.

Walker, E. L., & Connolly, E. L. (2008). Time to pump iron: Iron-deficiency-signaling mechanisms of higher plants. *Current Opinion in Plant Biology*, *11*(5), 530–535.

Zhao, N., Yu, G., Wang, Q., Wang, R., Zhang, J., Liu, C., & He, N. (2020). Conservative allocation strategy of multiple nutrients among major plant organs: From species to community. *Journal of Ecology*, *108*(1), 267–278.

Zahra, N., Hafeez, M. B., Shaukat, K., Wahid, A., & Hasanuzzaman, M. (2021). Fe toxicity in plants: Impacts and remediation. *Physiologia Plantarum*, *173*(1), 201–222.

How to cite this article: Gama, F., Saavedra, T., Dandlen, S., García-Caparrós, P., de Varennes, A., Nolasco, G., Correia, P. J., & Pestana, M. (2023). Silencing of *FRO1* gene affects iron homeostasis and nutrient balance in tomato plants. *Journal of Plant Nutrition and Soil Science*, 1–14. https://doi.org/10.1002/jpln.202300071